International Journal of Robotics and Control Systems
Vol. 6, No. 2, 2026, pp. 1181-1196
ISSN 2775-2658
http://pubs2.ascee.org/index.php/ijrcs

Optimizing Facial and Neck Muscle Signals Using Feature Extraction and Machine Learning for Assistive Device Control in Tetraplegia

Endro Yulianto [a,1], Lusiana [a,2,*], Triwiyanto [a,3], Putu Dody Surya Ananda [a,4]

[a] Department of Electro-medical Technology, Poltekkes Kemenkes Surabaya, Surabaya, Indonesia
[1] endro76@poltekkes-surabaya.ac.id; [2] lusiana.tekmed@poltekkes-surabaya.ac.id; [3] triwi@poltekkes-surabaya.ac.id;
[4] dodysurya03@gmail.com
* Corresponding Author

ARTICLE INFO

Article history
Received February 18, 2026
Revised April 10, 2026
Accepted April 18, 2026

Keywords
EMG;
Feature Extraction;
Tetraplegia;
Machine Learning

ABSTRACT

Tetraplegia is a neurological condition that causes paralysis of both upper and lower limbs, forcing affected individuals to rely almost entirely on facial and neck muscle movements to interact with their environment. This severe limitation reduces independence in daily activities and motivates the development of assistive technologies. One promising solution is the use of electromyography (EMG) signals generated by facial and neck muscle contractions as a human-computer interface for controlling external electronic devices. This study proposes reducing the number of EMG tapping points from four to three while maintaining four distinct command classes. This reduction poses a non-trivial challenge, as fewer channels generally decrease signal separability, increase feature overlap, and lead to higher classification ambiguity. In this research, EMG signals were acquired from six muscle channels, namely the Corrugator Supercilii, Temporalis, Zygomaticus, Orbicularis Oris, left Sternocleidomastoid (SCM) and right SCM. These muscles were activated through six intentional movements: brow furrowing, biting molars, grinning, kissing, looking right, and looking left. Feature extraction was performed using Mean Absolute Value (MAV) and Root Mean Square (RMS), while classification was conducted using Support Vector Machine (SVM) and Decision Tree (DT). Data were collected from ten participants using an instrumented tapping device, and signal processing and classification were implemented on a Raspberry Pi 4. The experimental results showed that three optimal tapping points, located at the right SCM, left SCM, and Zygomaticus muscles, were sufficient to represent four contraction commands corresponding to biting, grinning, looking right, and looking left. The DT classifier consistently outperformed SVM across all feature sets, achieving accuracies of 86.8% (MAV), 86.3% (RMS), and 86.9% (combined), compared to 84.2–84.6% for SVM. These results indicate that reducing the number of tapping points does not significantly degrade classification performance. In conclusion, the proposed EMG-based control system offers a simpler and more efficient human–computer interface for individuals with tetraplegia, enabling multi-command control with reduced hardware complexity.

1. Introduction

Recent advancements in Human–Machine Interface (HMI) systems have improved interaction between humans and electronic devices [1]–[5]. Modern HMI technologies integrate biological signals such as touch, speech, eye movement, and muscle activity to generate control commands for external systems [6]–[10]. Such developments are especially relevant for individuals with severe motor impairments caused by spinal cord injury (SCI), which can lead to paraplegia or tetraplegia. Individuals with tetraplegia experience paralysis of both upper and lower limbs, severely limiting their ability to perform daily activities independently [11]–[15]. Individuals with tetraplegia experience significant limitations in daily activities, reducing independence and quality of life [16]–[18]. Although assistive technologies have evolved rapidly in the past five years, many systems still rely on residual arm or hand function, making them unsuitable for users with complete upper-limb paralysis [19]–[22].

However, most existing EMG-based systems require multiple electrodes proportional to the number of command classes, increasing hardware complexity and reducing user comfort. This highlights the need for optimizing electrode configurations. Such systems should utilize preserved voluntary muscle activity from facial and neck muscles without requiring excessive sensor placement [23]–[26]. Electromyography (EMG) has emerged as a reliable bioelectrical signal for capturing muscle activation patterns and translating them into machine-interpretable commands [27]–[30]. Recent studies have explored the use of facial and neck EMG signals for assistive applications, including wheelchair navigation, robotic control, and human–computer interaction [31]–[35]. Compared with healthy individuals, people with SCI often retain greater voluntary control of facial and cervical muscles, making these signals a viable option for assistive control systems [36]–[38]. Recent investigations have utilized facial EMG for expression recognition, cursor movement, and communication aids with high classification accuracy using machine learning and deep learning approaches [39]–[42]. Similarly, neck EMG signals from the sternocleidomastoid muscle have been successfully employed for directional control in mobility assistance systems [43]–[45]. Common feature extraction methods include Mean Absolute Value (MAV) and Root Mean Square (RMS), while classifiers such as Support Vector Machine (SVM) and Decision Tree (DT) are widely used [46]–[48]. Various machine learning approaches have been applied to improve EMG signal classification performance [49], [50]. Several studies have reported multi-command EMG-based control systems using a limited number of electrodes [51]. Previous works have demonstrated three-command control using 2–3 facial or neck EMG channels; however, achieving four-command control typically requires four or more electrodes to maintain classification accuracy and robustness [52].

This study addresses this gap by analyzing six facial and neck muscles and identifying the three most representative channels for four-command external device control. The main contributions of this study are:

- Reducing EMG tapping points from four to three while maintaining four command classes.
- Identifying optimal electrode placements on facial and neck muscles.
- Evaluating classification performance using MAV, RMS, SVM, and DT.
- Demonstrating a low-complexity EMG-based system suitable for embedded implementation.

2. Method

2.1. Proposed Method

This study involved 10 human subjects aged 20–22 years, recruited from the Department of Electrical-Medical Engineering Technology, Poltekkes Kemenkes Surabaya. Ethical approval for this study was obtained from the Health Research Ethics Committee of Poltekkes Kemenkes Surabaya. All participants were informed about the study procedures and provided written informed consent prior to data collection. EMG signals were recorded from six electrode placement points using six EMG channels, as shown Fig. 1. In this case, the researchers were first recorded EMG signals at Six

EMG recording channels were used. CH1 was placed over the Corrugator Supercilii muscle, approximately 1–2 cm above the medial end of the eyebrow. CH2 was positioned on the Temporalis muscle, approximately 2–3 cm above the zygomatic arch along the anterior temporal region. CH3 was placed on the Zygomaticus muscle at the midline between the corner of the mouth and the zygomatic bone. CH4 was positioned over the Orbicularis Oris muscle, approximately 1 cm lateral to the mouth corner. CH5 and CH6 were placed on the left and right Sternocleidomastoid (SCM) muscles, approximately 3–5 cm above the clavicle along the muscle belly. All electrodes were aligned parallel to the muscle fiber orientation with an inter-electrode distance of approximately 2 cm. Surface electrodes were placed following the SENIAM recommendations and general clinical EMG guidelines as shown in Fig. 1. Furthermore, the signal used to record used Ag/AgCl type surface electrodes in order to detect muscle electrical activity (EMG) during contraction and relaxation [33], [34]. The EMG sensor was assembled using an instrumentation amplifier with a gain of 1000×, followed by a fourth-order Butterworth band-pass filter with a cut-off frequency of 79–480 Hz to isolate EMG signals. A 50 Hz notch filter was applied to suppress power-line interference. The filtered signal was then digitized using an MCP3008 analog-to-digital converter (ADC) with 10-bit resolution and a sampling rate of 1000 Hz, and processed on a Raspberry Pi 4 for feature extraction and classification [35]. IC MCP3008 was used as an analog-to-digital data converter (ADC) with the Raspberry Pi4 used as a microprocessor to process ADC data, and Python was used as a programming language.

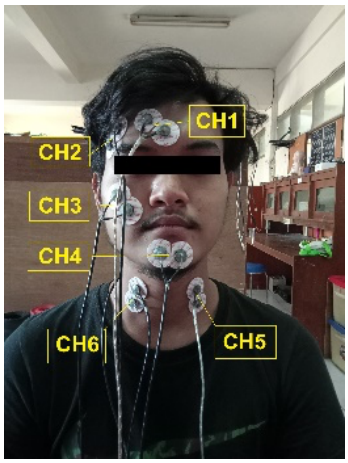

Fig. 1. Electrodes placement

EMG data were recorded using a sampling frequency of 1000Hz and then a windowing process was performed every 100ms which resulted in the extraction of the Mean Absolute Value (MAV) and Root Mean Square (RMS) feature extraction values [36]. EMG data were acquired from six intentional movements: frowning eyebrows (FE), biting (BITE), grinning (GRIN), kissing (KISS), looking right (LR), and looking left (LL). Each subject performed each movement in five repeated trials, with a relaxation period inserted between consecutive movements to reduce muscle carry-over effects. Thus, each class consisted of 50 trials in total (10 subjects × 5 repetitions), resulting in 300 trials across the six movement classes. To prevent data leakage and ensure fair evaluation, the dataset was divided into training and testing sets using an 80:20 ratio, where 80% of the data were used for training and 20% for testing. This split was used to evaluate the classification performance of the proposed system. Euclidean Distance (ED) was used as the channel selection criterion to quantify the separability of EMG features among movement classes. For each channel, the mean feature vector of each class was first calculated using the extracted MAV and RMS values. The ED was then computed between class centroids, and channels with larger average inter-class distances were considered to provide better discriminative information. Therefore, channels with the highest ED values were selected as the optimal tapping points for subsequent classification. ED was chosen because it is computationally simple, interpretable, and suitable for lightweight embedded implementation on Raspberry Pi shown in Fig. 2.

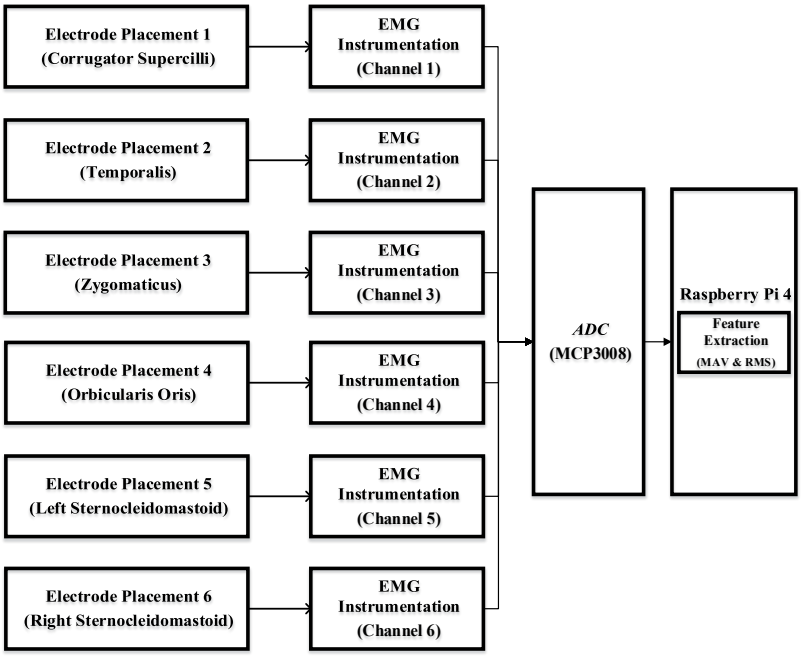

Fig. 2. Block diagram

Mean Absolute Value (MAV) is a formula for calculating mean values and windowing values calculated in absolute values. The MAV calculation as in (1):

$$MAV = \frac{1}{N}\sum_{I=1}^{N}|x_i| \tag{1}$$

In this case, N variable represents the amount of data and x_i represents the sequence of data a number of i. Furthermore, Root Mean Square (RMS) is the relationship between constant force and contraction without fatigue. The RMS formula as in (2):

$$RMS = \sqrt{\frac{1}{n}\sum_{I=1}^{N}{x_i}^2} \tag{2}$$

where N variable represents the amount of data and x_i represents the sequence of data a number of i. The average of the measurements was calculated as in (3):

$$\bar{X} = \frac{X_1 + X_2 \ldots X_n}{n} \tag{3}$$

where $\bar{X}$ indicates the mean value, X_1 indicates the value of the first measurement, X_2 indicates the value of the second measurement, and X_n indicates the value of the *n-th* measurement. Euclidean distance is one way to calculate the distance between two pieces of data in Euclidean space (including two-dimensional, three-dimensional, or more Euclidean fields). Evaluation of the degree of similarity of the data with the Euclidean Distance formula can be applied as in (4):

$$d_{ij} = \sqrt{\sum_{k=1}^{n}(x_{ik} - y_{jk})^2} \tag{4}$$

where d is the distance between i and j, i is the data center of j data on the attribute, k is the symbol of the data, n is the number of data, x_{ik} is the kth cluster data center, and y_{jk} is the data in each *k-th* data.

2.2. Machine Learning

Support Vector Machine (SVM) is used as a classification method to separate EMG signal patterns into predefined classes. It is selected due to its effectiveness in handling high-dimensional data [53]. Two classification algorithms were used in this study, namely Support Vector Machine (SVM) and Decision Tree (DT). SVM was employed to classify EMG feature patterns into predefined movement classes, while DT was used due to its low computational complexity and suitability for real-time implementation.

2.3. Decision Tree

Decision Tree (DT) was used as a lightweight classifier due to its low computational complexity and interpretability [54], [55].

2.4. Evaluation of Machine Learning Algorithms

The algorithm workflow consisted of five stages: (1) EMG signal acquisition from six channels, (2) signal segmentation using a 100 ms window, (3) feature extraction using MAV and RMS, (4) channel selection using Euclidean Distance, and (5) classification using SVM and DT. The dataset was then divided into training and testing sets, and classification accuracy was used to compare the performance of the evaluated models. Finally, the best-performing model was implemented for real-time control of the wheelchair prototype [56]–[58]. The overall workflow is illustrated in Fig. 2 and Fig. 3.

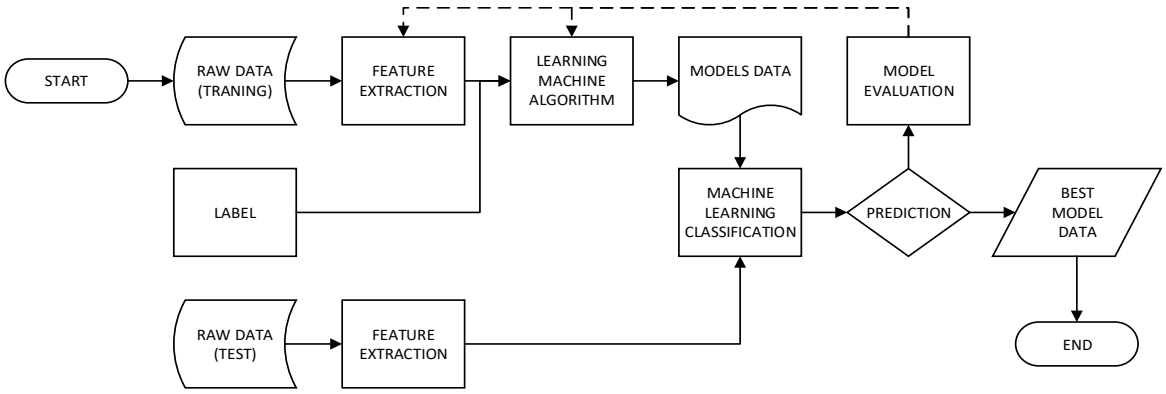

Fig. 3. Machine learning algorithm evaluation flowchart

2.5. Application of Machine Learning to Wheelchairs

After going through the analysis process, the Machine learning with the best accuracy is obtained and is applied to wheelchairs. Raw data is obtained from EMG signals that have gone through a series of instrumentation and then feature extraction is performed to produce extracted data along with the labels. The extracted data will be processed by machine learning and compared with the training data on the model. Then the data is classified based on 4 classes, namely forward, backward, turn right and turn left. If the data matches the class, Machine Learning will send serial data to the driver via Bluetooth to move the wheelchair. The results of the accuracy of the Machine learning can be known by calculating the number of movements tested with success according to their classification [59], [60].

3. Results and Discussion

3.1. Results

Machine learning performance evaluation is carried out by combining MAV and RMS feature extraction types with SVM and DT classification where the MAV&RMS-DT combination produces the highest accuracy of 86.9%. These results indicate that the proposed three-channel configuration is sufficient to achieve reliable multi-command classification while reducing hardware complexity compared to conventional multi-channel systems. The results of the machine learning model were tested directly to move the wheelchair forward, backward, turn right and turn left resulting in a total average accuracy of 84.8%. The real-time wheelchair testing was conducted using a total of 20 trials for each command. The success rate was calculated as the ratio of correctly executed commands to the total number of trials. The system achieved an average success rate of 84.8%, indicating reliable real-time performance. This result can be explained by the functional roles of the selected muscles. The sternocleidomastoid (SCM) muscles (CH5 and CH6) are primarily responsible for head rotation, which produces distinct EMG activation patterns for left and right movements. Meanwhile, the Zygomaticus muscle (CH3) is strongly associated with facial expressions such as grinning. These distinct physiological activation patterns reduce overlap between classes, allowing three channels to preserve sufficient discriminative information for four-command classification.

The calculation of the ED value was carried out using Python on the Raspberry Pi4 where the six movements on each channel were compared one by one so that the ED value of each movement was obtained with 15 movement combinations for each channel. The ED value later was used to show the movement relationship in each channel. The greater the ED value, the greater the separation of the two variables.

The ED value at CH 1 as presented in Fig. 4 shows that the FE movement had a large value compared to other movements with a mean value of 2301.44 (MAV) and 2461.65 (RMS). On the other hand, the BITE movement also had a large value compared to other movements with an average of 1116 (MAV) and 1296.51 (RMS) but it was not greater than the FE movement and had data that was quite significantly separated from the FE movement (FE-BITE), namely 1692.78 (MAV) and 3127.68 (RMS).

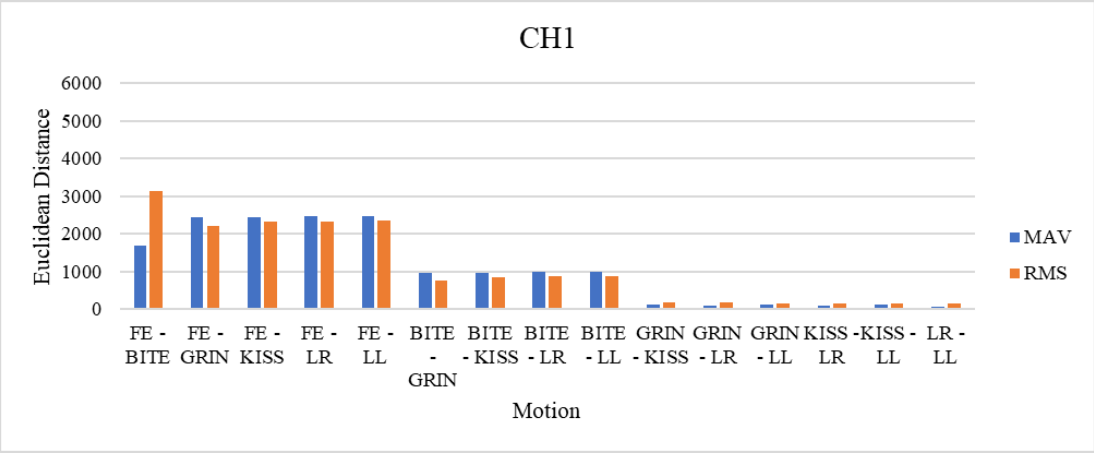

Fig. 4. Euclidean distance channel 1

Fig. 5 is the ED value of CH 2 where the BITE movement had a very large value compared to other movements. the average ED value obtained in the BITE movement in CH 2 is 4496.41 (MAV) and 5779.96 (RMS). Since no other movement has a high ED value, the BITE Movement is the dominant move in this CH2. The value of ED CH 3 which can be seen in Fig. 6 shows that the GRIN and BITE movements had a large value compared to other movements with GRIN movement averages of 2521.53 (MAV) and 3178.33 (RMS) and BITE movements of 2222.43 (MAV) and 2772.84 (RMS). This proved that in CH 3, 2 movements produced EMG signal activation, namely the GRIN and BITE

movements with the GRIN movement having a more dominant position than the BITE movement that can be seen from the larger ED value. Although CH 3 was affected by 2 different movements, the GRIN and BITE movements still had significant separate data with ED values 2017.26 (MAV) and 2502.11 (RMS) so that they can be easily classified using machine learning.

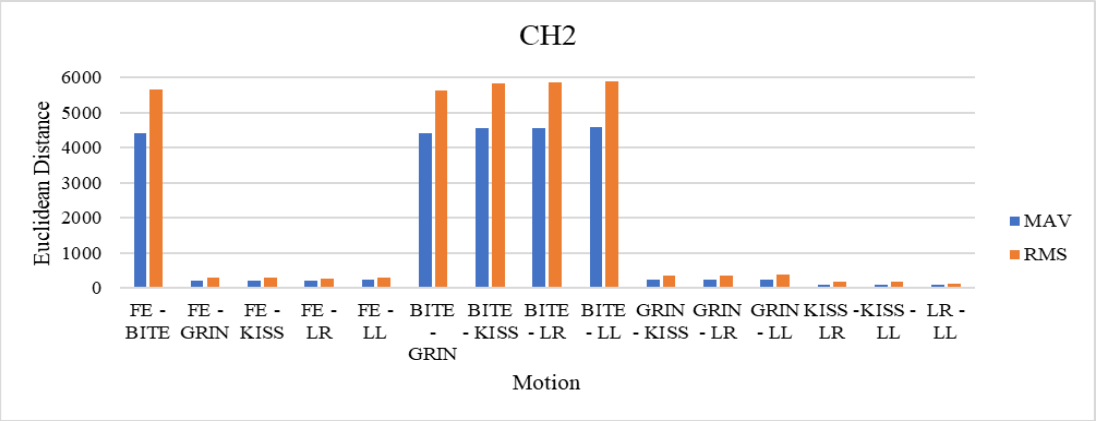

Fig. 5. Euclidean distance channel 2

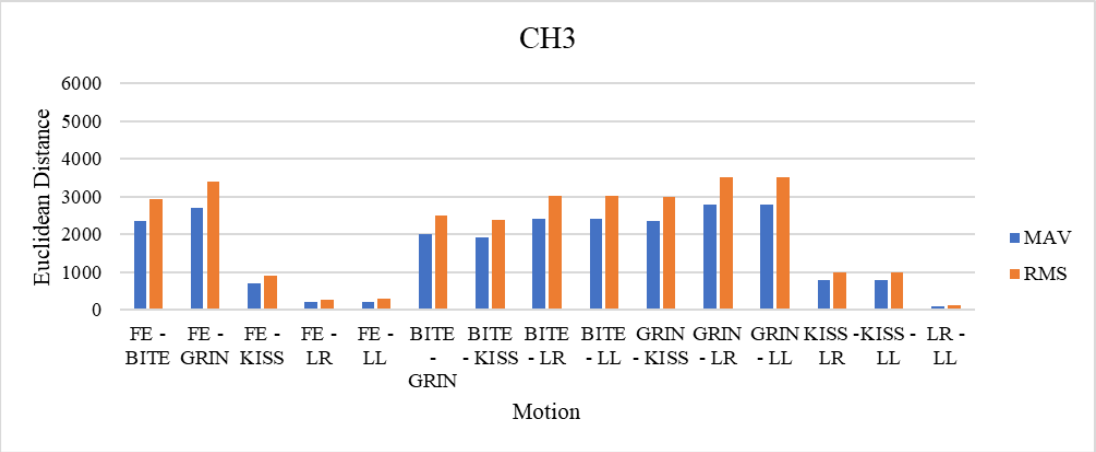

Fig. 6. Euclidean distance channel 3

Fig. 7 is the ED value of CH 4 where the KISS and GRIN movements had a large value compared to other movements with KISS movement averages of 3864.60 (MAV) and 4786.97 (RMS) and GRIN movements of 3172.21 (MAV) and 3941.27 (RMS). This proved that in CH 4, 2 movements produced EMG signal activation, namely the KISS and GRIN movements with the KISS movement having a more dominant position than the GRIN movement that can be seen from the larger ED value. Although CH4 was influenced by 2 different movements, the GRIN and BITE movements still had significant separate data with ED values of 2974.38 (MAV) and 3709.29 (RMS) so that they can be easily classified using machine learning. This confirms that optimized feature selection directly improves classification reliability for assistive interfaces. However, at CH 4 only 3 out of 10 respondents had an EMG signal activation value with GRIN movement which made the GRIN movement in CH 4 not appear significant even though the movement had a large ED value compared to other movements.

The same thing as CH 2 can be seen in CH5 as Fig. 8, the ED value of CH 5 where the LR movement had a very large value compared to other movements. the average ED value obtained in the LR movement in CH 5 is 3602.86 (MAV) and 4511.11 (RMS). Since no other movement has a high ED value, the LR Movement is the dominant move in this CH5. Fig. 9 shows the ED value of CH 6 where the LL movement had a very large value compared to other movements. the average ED value obtained in the LL movement in CH 6 is 4035.28 (MAV) and 5015.59 (RMS). Since no other movement has a high ED value, the LL Movement is the dominant move in this CH6.

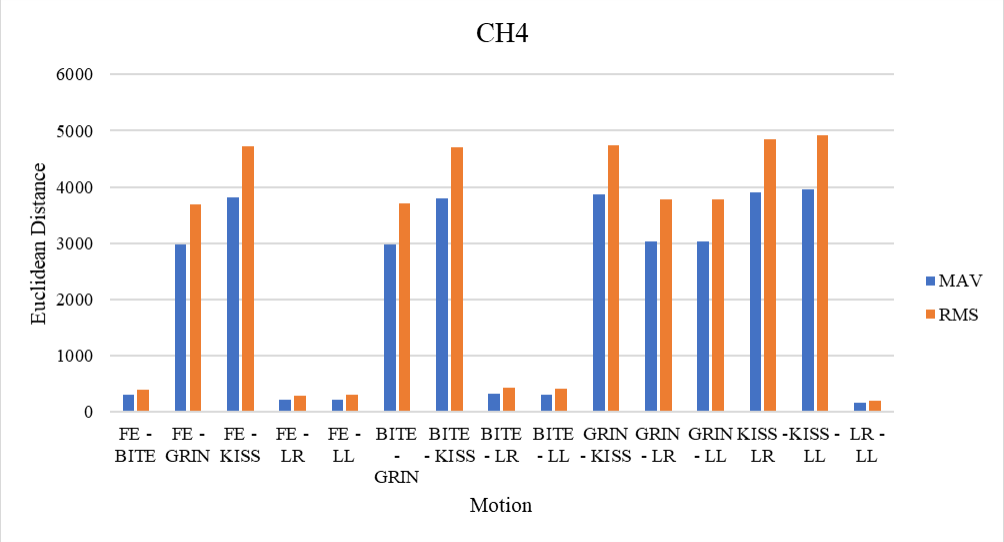

Fig. 7. Euclidean distance channel 4

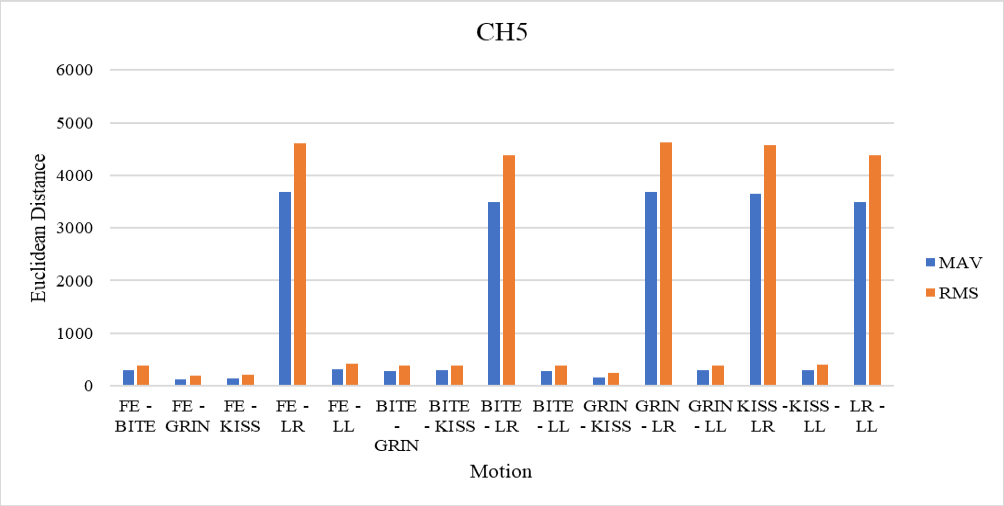

Fig. 8. Euclidean distance channel 5

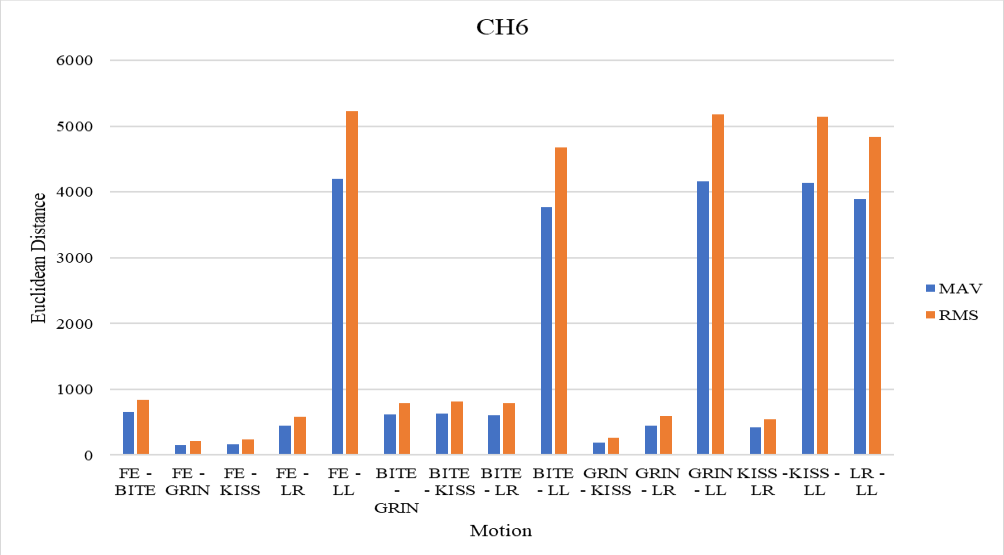

Fig. 9. Euclidean distance channel 6

From the graphs on CH 1 to CH 6 it is found that the channels that have 2 dominant movements are CH 2, CH 3, and CH 4. The experimental results using 10 respondents in CH 4 for the 6 movements given. Of the 10 respondents, there were 4 respondents who succeeded in showing results against the KISS and GRIN movements.

The data that has been taken will be labeled according to the movements carried out then split with a percentage of 80% as test data and 20% as training data taken from the total data. Next, the extracted features were used to train machine learning models using two classification algorithms: Support Vector Machine (SVM) and Decision Tree (DT). The SVM classifier employed a Radial Basis Function (RBF) kernel with default regularization parameters, while the Decision Tree classifier was configured with a maximum depth of 10 to prevent overfitting. Model performance was evaluated using 5-fold cross-validation to ensure robustness and generalization. Class distribution was balanced during training to avoid bias toward dominant classes. The results of machine learning performance measurements can be seen in the following Table 1. presents the classification performance results. While an ablation study comparing six-channel, four-channel, and three-channel configurations would provide a more comprehensive evaluation, the current work focuses on identifying an optimal minimal-channel configuration. Therefore, a detailed ablation analysis will be considered in future work to further validate the effectiveness of channel reduction.

It should be noted that the reported accuracy is based on a subject-dependent data split, which may lead to optimistic performance estimation due to potential overlap of subject-specific patterns between training and testing data. To validate the robustness of the proposed model, cross-validation was performed using repeated random splits of the dataset. The results showed consistent performance across different splits, indicating that the model is stable and not significantly affected by data partitioning.

In addition to overall accuracy, class-wise performance was evaluated using confusion matrix analysis. The results indicate that directional commands (LR and LL) achieved higher classification accuracy compared to facial expression-based commands due to more distinct muscle activation patterns. Misclassifications primarily occurred between facial expressions such as GRIN and BITE, which share partially overlapping muscle activations.

Table 1. Machine learning accuracy results 80% Training Data 20% Test Data

Test	MAV (%)		RMS (%)		MAV-RMS (%)	
	DT	SVM	DT	SVM	DT	SVM
Mean	86.8	84.5	86.3	84.2	86.9	84.6
Standard Deviation	0.8	0.7	0.5	0.4	0.7	0.7

The data that was trained amounted to 12016 data from 80% of the data from 10 respondents (8 sets of movements for each respondent). While the test data amounted to 3005 data from 20% of the data from 10 respondents (2 sets of movements for each respondent). The test data will be entered into the machine learning algorithm to be classified by each method and repeated 10 times. The results of machine learning accuracy using different feature extraction methods are shown in Fig. 10. The Decision Tree (DT) classifier achieved higher performance compared to SVM across all feature sets, with the highest accuracy obtained using the combined MAV-RMS features. While these results demonstrate promising classification performance. A statistical comparison using ANOVA or t-tests would provide further validation of the significance of performance differences. Additionally, a comparative ablation analysis across different channel configurations (e.g., 6-channel, 4-channel, and 3-channel) would further strengthen the evaluation. These analyses will be considered in future work.

3.2. Discussion

The relationship of the separateness of the movement data on each channel can be analyzed using ED calculations to find the relationship between movements to the channel because the ED method was a simple method to find the relationship of data separation [38]. Research showed that the

movement that has been done can produce EMG activity in one or two channels. This can be seen in Table 2.

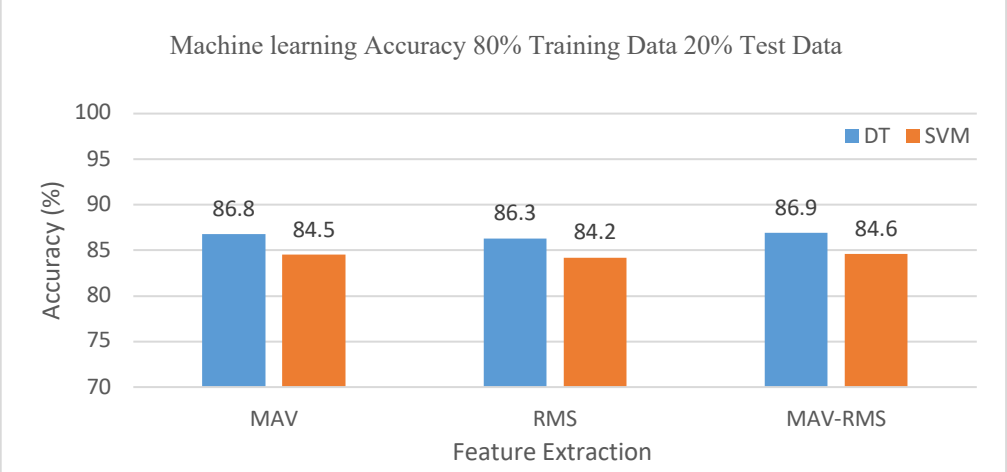

Fig. 10. Machine learning accuracy 80% Training Data 20% Test Data

Table 2. Dominant motion on each channel based on ED value

Channel	CH1		CH2	CH3		CH4		CH5	CH6
Motion (dominant)	FE	BITE	BITE	GRIN	BITE	KISS	GRIN	LR	LL
Average ED (MAV)	2301.44	1116	4496.41	2521.53	2222.43	3864.60	3172.21	3602.86	4035.28
Average ED (RMS)	2461.65	1296.51	5779.96	3178.33	2772.84	4786.97	3941.27	4511.11	5015.59
ED Value Between Motion (MAV)	1692.78	-	-	2017.26	-	2974.38	-	-	-
ED Value Between Motion (RMS)	3127.68	-	-	2502.11	-	3709.29	-	-	-

Based on Table 3, the Corrugator Supercilli (CH 1), Zygomaticus (CH 3) and Orbicularis Oris (CH 4) muscles produced 2 dominant movements with a higher ED value than the other movements. the two dominant movements in each channel are searched for the relationship of separation using the ED value. From this it can be seen that the relationship of the greatest separation between the two dominant movements is shown in CH 4. because it has the largest ED value between the two dominant movements. CH 4 had greater separation of the 2 dominant movements than CH 1 and CH 3. After but not all of the respondents resulted in activation of the GRIN movement in CH 4. In addition, the Temporal (CH 2), Left SCM (CH 5), and Right SCM (CH 6) only had 1 dominant move with a large ED value compared to other moves. CH 2 is dominant with the BITE movement. CH 5 is dominant with the LR movement. CH 6 is dominant with the LL movement. The same thing was also found in Hess's research which showed that the Corrugator Supercilli, Zygomaticus, and Orbicularis Oris muscles were affected by facial expressions when happy, sad, disgusted, and angry. Movements and expressions generated from these facial muscles can be distinguished using machine learning classification. Furthermore, the classification can be implemented into the Human-Computer Interface (HCI).

The main findings of this study demonstrate that RMS-based feature extraction produces higher Euclidean Distance (ED) values than MAV, indicating greater class separability and improved classification performance. This suggests that RMS features are more effective in distinguishing muscle activation patterns, thereby facilitating more accurate machine learning classification. Furthermore, the results confirm that three optimized EMG tapping points—located at the right

sternocleidomastoid, left sternocleidomastoid, and zygomaticus muscles—are sufficient to represent four distinct command classes. This reduction in the number of sensing channels simplifies hardware requirements and improves user comfort without compromising system accuracy. These findings are consistent with previous research, which also reported superior performance of RMS features compared to other time-domain features such as MAV, VAR, and SSI for EMG-based motion classification.

Table 3. Total ED value of each channel

Channel	Feature Extraction	
	MAV	RMS
CH1	15985.28	16615.03
CH2	24327.50	31593.66
CH3	24457.34	30803.71
CH4	32858.58	40925
CH5	20531.97	25955.40
CH6	24509.33	30768.07
Total	142670	176661

The implications of these findings suggest that efficient feature selection and optimized sensor placement can significantly enhance the practicality of EMG-based assistive technologies. By reducing the number of electrodes while maintaining classification accuracy, the proposed approach improves usability and supports the development of more compact and comfortable assistive devices for individuals with tetraplegia. The strengths of this study include the successful implementation of a simplified EMG configuration and validation using embedded machine learning on a low-cost platform. However, the study has several limitations such as this study did not analyze muscle fatigue effects and only involved healthy participants, which may limit generalizability. Muscle fatigue, which may influence EMG signal characteristics, was not analyzed in this work. Additionally, the experimental data were obtained from healthy participants rather than individuals with tetraplegia. Future research should address these limitations by incorporating fatigue analysis and validating the system with target users to ensure real-world applicability and robustness.

4. Conclusion

This study demonstrates that three EMG channels from facial and neck muscles are sufficient to represent four control commands, achieving a classification accuracy of 86.9%. This result confirms that channel reduction can be achieved without significantly degrading classification performance. However, this study has several limitations. First, the evaluation was conducted using healthy participants rather than individuals with tetraplegia, which may limit the applicability of the results to the target population. Second, the current system is not yet suitable for safety-critical applications such as direct wheelchair control, as misclassification may result in unintended movements. Therefore, practical deployment requires additional validation, improved classification reliability, and the integration of fail-safe control mechanisms. Future work will focus on subject-independent evaluation using cross-validation, testing on individuals with tetraplegia, and the development of more robust classification strategies, such as adaptive feature selection and real-time error correction mechanisms.

The theoretical contribution of this study lies in demonstrating that optimized EMG channel selection, combined with lightweight feature extraction and machine learning, can achieve reliable multi-command control while reducing sensor requirements. This approach contributes new knowledge toward the design of efficient and user-friendly EMG-based assistive technologies. However, this study has several limitations, including the absence of muscle fatigue analysis and the use of healthy participants rather than individuals with tetraplegia. Future work should incorporate fatigue evaluation, explore additional feature extraction and deep learning techniques, and validate the proposed system using participants with tetraplegia to ensure real-world applicability and robustness.

Further investigation into adaptive algorithms and long-term usability is also encouraged to support the development of practical assistive solutions.

Supplementary Materials: The following supporting information can be downloaded at: https://drive.google.com/drive/folders/1LrSa4jzWMfTsbN1ZiIW3RUayVrtXfs_q?usp=sharing

Author Contribution: All authors contributed equally to the main contributor to this paper. All authors read and approved the final paper.

Funding: This research was funded by DIPA UPPM Poltekkes Kemenkes Surabaya

Acknowledgment: The authors would like to thank all the laboratory member of Departement of Electro-medical Technology Poltekkes Kemenkes Surabaya,for supporting this research work.

Conflicts of Interest: The authors declare no conflict of interest

References

[1] D. Esposito, J. Centracchio, E. Andreozzi, G. D. Gargiulo, G. R. Naik, and P. Bifulco, "Biosignal-based human-machine interfaces for assistance and rehabilitation: A survey," *Sensors*, vol. 21, no. 20, p. 6863, 2021, https://doi.org/10.3390/s21206863.

[2] E. B. Küçüktabak, S. J. Kim, Y. Wen, K. Lynch, and J. L. Pons, "Human-machine-human interaction in motor control and rehabilitation: A review," *Journal of NeuroEngineering and Rehabilitation*, vol. 18, no. 1, p. 183, 2021, https://doi.org/10.1186/s12984-021-00974-5.

[3] S. Ventura, G. Ottoboni, A. Pappadà, and A. Tessari, "Acceptance of assistive technology by users with motor disabilities due to spinal cord or acquired brain injuries: A systematic review," *Journal of Clinical Medicine*, vol. 12, no. 8, p. 2962, 2023, https://doi.org/10.3390/jcm12082962.

[4] S. M. Ali, S. Noghanian, Z. U. Khan, S. Alzahrani, S. Alharbi, M. Alhartomi, and R. Alsulami, "Wearable and flexible sensor devices: Recent advances in designs, fabrication methods, and applications," *Sensors*, vol. 25, no. 5, p. 1377, 2025, https://doi.org/10.3390/s25051377.

[5] Y. Sun, X. Chen, B. Liu, L. Liang, Y. Wang, S. Gao, and X. Gao, "Signal acquisition of brain-computer interfaces: A medical-engineering crossover perspective review," *Fundamental Research*, vol. 5, no. 1, pp. 3–16, 2025, https://doi.org/10.1016/j.fmre.2024.04.011.

[6] H. Su, W. Qi, J. Chen, C. Yang, J. Sandoval, and M. A. Laribi, "Recent advancements in multimodal human-robot interaction," *Frontiers in Neurorobotics*, vol. 17, p. 1084000, 2023, https://doi.org/10.3389/fnbot.2023.1084000.

[7] A. Palumbo, V. Gramigna, B. Calabrese, and N. Ielpo, "Motor-imagery EEG-based BCIs in wheelchair movement and control: A systematic literature review," *Sensors*, vol. 21, no. 18, p. 6285, 2021, https://doi.org/10.3390/s21186285.

[8] Z. Yang, D. Jiang, Y. Sun, B. Tao, X. Tong, and G. Jiang, "Dynamic gesture recognition using surface EMG signals based on multi-stream residual network," *Frontiers in Bioengineering and Biotechnology*, vol. 9, p. 779353, 2021, https://doi.org/10.3389/fbioe.2021.779353.

[9] B. H. Quan, N. D. T. Anh, H. V. Phi, and B. T. Thanh, "Redesigning multimodal interaction: Adaptive signal processing and cross-modal interaction for hands-free computer interaction," *Sensors*, vol. 25, no. 17, p. 5411, 2025, https://doi.org/10.3390/s25175411.

[10] J. F. Castruita-López, M. Aviles, D. C. Toledo-Pérez, I. Macías-Socarrás, and J. Rodríguez-Reséndiz, "Electromyography signals in embedded systems: A review of processing and classification techniques," *Biomimetics*, vol. 10, no. 3, p. 166, 2025, https://doi.org/10.3390/biomimetics10030166.

[11] Y. Liu, X. Yang, and Z. He, "Spinal cord injury: Global burden from 1990 to 2019 and projections up to 2030 using Bayesian age-period-cohort analysis," *Frontiers in Neurology*, vol. 14, p. 1304153, 2023, https://doi.org/10.3389/fneur.2023.1304153.

[12] M. Chiappalone, V. R. Cota, M. Carè, M. Di Florio, R. Beaubois, S. Buccelli, F. Barban, M. Brofiga, A. Averna, F. Bonacini, et al., "Neuromorphic-based neuroprostheses for brain rewiring: State-of-the-art and perspectives in neuroengineering," *Brain Sciences*, vol. 12, no. 11, p. 1578, 2022, https://doi.org/10.3390/brainsci12111578.

[13] A. Korik, K. McCreadie, N. McShane, N. Du Bois, M. Khodadadzadeh, J. Stow, J. McElligott, Á. Carroll, and D. Coyle, "Competing at the Cybathlon championship for people with disabilities: Long-term motor imagery brain-computer interface training of a cybathlete who has tetraplegia," *Journal of NeuroEngineering and Rehabilitation*, vol. 19, no. 1, p. 95, 2022, https://doi.org/10.1186/s12984-022-01073-9.

[14] J. Hodel, C. Sabariego, M. Galvis Aparicio, A. Scheel-Sailer, V. Seijas, and C. Ehrmann, "Revisiting functioning recovery in persons with spinal cord injury undergoing first rehabilitation: Trajectory and network analysis of a Swiss cohort study," *PLOS ONE*, vol. 19, no. 2, p. e0297682, 2024, https://doi.org/10.1371/journal.pone.0297682.

[15] K. S. Adewole, A. Jacobsson, and P. Davidsson, "Intrusion detection framework for Internet of Things with rule induction for model explanation," *Sensors*, vol. 25, no. 6, p. 1845, 2025, https://doi.org/10.3390/s25061845.

[16] K. Kovacs Burns, Z. Bhatia, B. Gill, D. van der Nest, J. Knox, M. Mouneimne, T. Buck, R. Charbonneau, K. Aiello, A. Loyola Sanchez, et al., "Measures for persons with spinal cord injury to monitor their transitions in care, health, function, and quality of life experiences and needs: A protocol for co-developing a self-evaluation tool," *Healthcare*, vol. 12, no. 5, p. 527, 2024, https://doi.org/10.3390/healthcare12050527.

[17] J. M. Kijiru, W. M. Karuguti, N. Kingau, and E. Atieno, "Met and unmet assistive technology needs, participations restrictions and quality of life of spinal cord injury survivors: Systematic review," *Bulletin of Faculty of Physical Therapy*, vol. 31, no. 1, p. 2, 2026, https://doi.org/10.1186/s43161-025-00335-6.

[18] E. Nunez Sardinha, N. Zook, D. Western, F. Niyi-Odumosu, V. Ruiz Garate, and M. Múnera, "Effectiveness and acceptance of assistive technologies for people with tetraplegia: A systematic review," *Assistive Technology*, vol. 38, no. 2, pp. 87–107, 2026, https://doi.org/10.1080/10400435.2025.2540119.

[19] M. Bonanno, B. Saracino, I. Ciancarelli, G. Panza, A. Manuli, G. Morone, and R. S. Calabrò, "Assistive technologies for individuals with a disability from a neurological condition: A narrative review on the multimodal integration," *Healthcare*, vol. 13, no. 13, p. 1580, 2025, https://doi.org/10.3390/healthcare13131580.

[20] B. Maiseli, A. T. Abdalla, L. V. Massawe, M. Mbise, K. Mkocha, N. A. Nassor, M. Ismail, J. Michael, and S. Kimambo, "Brain-computer interface: Trend, challenges, and threats," *Brain Informatics*, vol. 10, no. 1, p. 20, 2023, https://doi.org/10.1186/s40708-023-00199-3.

[21] D. Farina, R. Merletti, and R. M. Enoka, "The extraction of neural strategies from the surface EMG: An update," *Journal of Applied Physiology*, vol. 117, no. 11, pp. 1215–1230, 2014, https://doi.org/10.1152/japplphysiol.00162.2014.

[22] Z. Zheng, Z. Wu, R. Zhao, Y. Ni, X. Jing, and S. Gao, "A review of EMG-, FMG-, and EIT-based biosensors and relevant human-machine interactivities and biomedical applications," *Biosensors*, vol. 12, no. 7, p. 516, 2022, https://doi.org/10.3390/bios12070516.

[23] H. Wang, S. Zuo, M. Cerezo-Sánchez, N. G. Arekhloo, K. Nazarpour, and H. Heidari, "Wearable super-resolution muscle-machine interfacing," *Frontiers in Neuroscience*, vol. 16, p. 1020546, 2022, https://doi.org/10.3389/fnins.2022.1020546.

[24] N. Mueller, V. Trentzsch, R. Grassme, O. Guntinas-Lichius, G. F. Volk, and C. Anders, "High-resolution surface electromyographic activities of facial muscles during mimic movements in healthy adults: A prospective observational study," *Frontiers in Human Neuroscience*, vol. 16, p. 1029415, 2022, https://doi.org/10.3389/fnhum.2022.1029415.

[25] V. Trentzsch, N. Mueller, M. Heinrich, A.-M. Kuttenreich, O. Guntinas-Lichius, G. F. Volk, and C. Anders, "Test-retest reliability of high-resolution surface electromyographic activities of facial muscles

during facial expressions in healthy adults: A prospective observational study," *Frontiers in Human Neuroscience*, vol. 17, p. 1126336, 2023, https://doi.org/10.3389/fnhum.2023.1126336.

[26] C. M. M. Queiroz, G. M. da Silva, S. Walter, L. B. Peres, L. M. D. Luiz, S. C. Costa, K. C. de Faria, A. A. Pereira, M. F. Vieira, A. M. Cabral, and A. O. Andrade, "Single channel approach for filtering electroencephalographic signals strongly contaminated with facial electromyography," *Frontiers in Computational Neuroscience*, vol. 16, p. 822987, 2022, https://doi.org/10.3389/fncom.2022.822987.

[27] C. R. Carvalho, J. M. Fernández, A. J. del-Ama, F. Oliveira Barroso, and J. C. Moreno, "Review of electromyography onset detection methods for real-time control of robotic exoskeletons," *Journal of NeuroEngineering and Rehabilitation*, vol. 20, no. 1, p. 141, 2023, https://doi.org/10.1186/s12984-023-01268-8.

[28] B. Zhu, D. Zhang, Y. Chu, X. Zhao, L. Zhang, and L. Zhao, "Face-computer interface (FCI): Intent recognition based on facial electromyography (fEMG) and online human-computer interface with audiovisual feedback," *Frontiers in Neurorobotics*, vol. 15, p. 692562, 2021, https://doi.org/10.3389/fnbot.2021.692562.

[29] A. C. Manero, S. L. McLinden, J. Sparkman, and B. Oskarsson, "Evaluating surface EMG control of motorized wheelchairs for amyotrophic lateral sclerosis patients," *Journal of NeuroEngineering and Rehabilitation*, vol. 19, no. 1, p. 88, 2022, https://doi.org/10.1186/s12984-022-01066-8.

[30] Z. Chen, H. Min, D. Wang, Z. Xia, F. Sun, and B. Fang, "A review of myoelectric control for prosthetic hand manipulation," *Biomimetics*, vol. 8, no. 3, p. 328, 2023, https://doi.org/10.3390/biomimetics8030328.

[31] D. V. D. S. Welihinda, L. K. P. Gunarathne, H. M. K. K. M. B. Herath, S. L. P. Yasakethu, N. Madusanka, and B.-I. Lee, "EEG and EMG-based human-machine interface for navigation of mobility-related assistive wheelchair (MRA-W)," *Heliyon*, vol. 10, no. 6, p. e27777, 2024, https://doi.org/10.1016/j.heliyon.2024.e27777.

[32] P. Chandania and P. Mahajani, "Machine learning-based classification of neck movements using sEMG and STM32 microcontroller," *International Journal of Microsystems and IoT*, vol. 3, no. 6, pp. 1693–1699, 2025, https://doi.org/10.5281/zenodo.18153231.

[33] G. Figas, A. Hadamus, M. Błażkiewicz, and J. Kujawa, "Symmetry of the neck muscles' activity in the electromyography signal during basic motion patterns," *Sensors*, vol. 23, no. 8, p. 4170, 2023, https://doi.org/10.3390/s23084170.

[34] A. M. Alqudah and Z. Moussavi, "Bridging signal intelligence and clinical insight: A comprehensive review of feature engineering, model interpretability, and machine learning in biomedical signal analysis," *Applied Sciences*, vol. 15, no. 22, p. 12036, 2025, https://doi.org/10.3390/app152212036.

[35] Q. Zhang, N. Fragnito, J. R. Franz, and N. Sharma, "Fused ultrasound and electromyography-driven neuromuscular model to improve plantarflexion moment prediction across walking speeds," *Journal of NeuroEngineering and Rehabilitation*, vol. 19, no. 1, p. 86, 2022, https://doi.org/10.1186/s12984-022-01061-z.

[36] L. García-Alén, A. Ros-Alsina, L. Sistach-Bosch, M. Wright, and H. Kumru, "Noninvasive electromagnetic neuromodulation of the central and peripheral nervous system for upper-limb motor strength and functionality in individuals with cervical spinal cord injury: A systematic review and meta-analysis," *Sensors*, vol. 24, no. 14, p. 4695, 2024, https://doi.org/10.3390/s24144695.

[37] N. Verma, J. Oh, E. Bedoy, N. Chetty, A. G. Steele, S. J. Park, J. R. Guerrero, A. H. Faraji, D. Weber, and D. G. Sayenko, "Transcutaneous stimulation of the cervical spinal cord facilitates motoneuron firing and improves hand-motor function after spinal cord injury," *Journal of Neurophysiology*, vol. 134, no. 1, pp. 128–143, 2025, https://doi.org/10.1152/jn.00422.2024.

[38] S. Hong, H. Kim, J. Ahn, and W. Park, "Influence of time since injury and physical activity level on upper limb kinematics and muscle activation during wheelchair propulsion in complete T12/L1 spinal cord injury," *BMC Musculoskeletal Disorders*, vol. 26, no. 1, p. 807, 2025, https://doi.org/10.1186/s12891-025-08987-0.

[39] J. P. Vásconez, L. I. Barona López, Á. L. Valdivieso Caraguay, and M. E. Benalcázar, "Hand gesture recognition using EMG-IMU signals and deep Q-networks," *Sensors*, vol. 22, no. 24, p. 9613, 2022, https://doi.org/10.3390/s22249613.

[40] N. Satterlee, X. Zuo, K. Moon, S. Q. Lee, M. Peterson, and J. S. Kang, "Sentence-level silent speech recognition using a wearable EMG/EEG sensor system with AI-driven sensor fusion and language model," *Sensors*, vol. 25, no. 19, p. 6168, 2025, https://doi.org/10.3390/s25196168.

[41] J. Li, S. Tang, and J. Guo, "Noise-adaption extended Kalman filter based on deep deterministic policy gradient for maneuvering targets," *Sensors*, vol. 22, no. 14, p. 5389, 2022, https://doi.org/10.3390/s22145389.

[42] R. F. Alqadda, F. B. Alhumaidi, K. H. Alsadah, D. D. Alahmari, M. M. Hegazi, and I. A. Aljamaan, "Wearable electromyography (EMG) and accelerometer device based on human-computer interaction for tetraplegic users," *Results in Engineering*, vol. 29, p. 108633, 2026, https://doi.org/10.1016/j.rineng.2025.108633.

[43] J. K. Muguro, P. W. Laksono, W. Rahmaniar, W. Njeri, Y. Sasatake, M. S. Ab Suhaimi, K. Matsushita, M. Sasaki, M. Sulowicz, and W. Caesarendra, "Development of surface EMG game control interface for persons with upper limb functional impairments," *Signals*, vol. 2, no. 4, pp. 834–851, 2021, https://doi.org/10.3390/signals2040048.

[44] J. Zhang, S. Huang, J. Li, Y. Wang, Z. Dong, and S.-J. Wang, "A perifacial EMG acquisition system for facial-muscle-movement recognition," *Sensors*, vol. 23, no. 21, p. 8758, 2023, https://doi.org/10.3390/s23218758.

[45] C. Li, Y. Xu, T. Feng, M. Wang, X. Zhang, L. Zhang, R. Cheng, W. Chen, W. Chen, and S. Zhang, "Fusion of EEG and EMG signals for detecting pre-movement intention of sitting and standing in healthy individuals and patients with spinal cord injury," *Frontiers in Neuroscience*, vol. 19, p. 1532099, 2025, https://doi.org/10.3389/fnins.2025.1532099.

[46] B. Chen, C. Chen, J. Hu, T. Nguyen, J. Qi, B. Yang, D. Chen, Y. Alshahrani, Y. Zhou, A. Tsai, T. Frush, and H. Goitz, "A real-time EMG-based fixed-bandwidth frequency-domain embedded system for robotic hand," *Frontiers in Neurorobotics*, vol. 16, p. 880073, 2022, https://doi.org/10.3389/fnbot.2022.880073.

[47] K. G. Rabe and N. P. Fey, "Evaluating electromyography and sonomyography sensor fusion to estimate lower-limb kinematics using Gaussian process regression," *Frontiers in Robotics and AI*, vol. 9, p. 716545, 2022, https://doi.org/10.3389/frobt.2022.716545.

[48] C. L. Kok, C. K. Ho, F. K. Tan, and Y. Y. Koh, "Machine learning-based feature extraction and classification of EMG signals for intuitive prosthetic control," *Applied Sciences*, vol. 14, no. 13, p. 5784, 2024, https://doi.org/10.3390/app14135784.

[49] J. Wang, D. Cao, J. Wang, and C. Liu, "Action recognition of lower limbs based on surface electromyography weighted feature method," *Sensors*, vol. 21, no. 18, p. 6147, 2021, https://doi.org/10.3390/s21186147.

[50] M. R. K. Kadavath, M. Nasor, and A. Imran, "Enhanced hand gesture recognition with surface electromyogram and machine learning," *Sensors*, vol. 24, no. 16, p. 5231, 2024, https://doi.org/10.3390/s24165231.

[51] T. Talaei Khoei, H. Ould Slimane, and N. Kaabouch, "Deep learning: Systematic review, models, challenges, and research directions," *Neural Computing and Applications*, vol. 35, no. 31, pp. 23103–23124, 2023, https://doi.org/10.1007/s00521-023-08957-4.

[52] J. M. Lopez-Villagomez, J. M. Lopez-Hernandez, R. I. Mata-Chavez, C. Rodriguez-Donate, Y. Guzman-Castro, and E. Cabal-Yepez, "Comparative evaluation of EMG signal classification techniques across temporal, frequency, and time-frequency domains using machine learning," *Applied Sciences*, vol. 16, no. 2, p. 1058, 2026, https://doi.org/10.3390/app16021058.

[53] Y. Zhang, Y. Liu, and X. Yang, "Review of support vector machine theory and application," *International Core Journal of Engineering*, vol. 7, no. 6, pp. 417–422, 2021, https://doi.org/10.6919/ICJE.202106_7(6).0049.

[54] I. D. Mienye and N. Jere, "A survey of decision trees: Concepts, algorithms, and applications," *IEEE Access*, vol. 12, pp. 86716–86727, 2024, https://doi.org/10.1109/ACCESS.2024.3416838.

[55] Z. Cui, X. Fu, X. Wan, J. Li, W. Chen, S. Zhu, and Y. Li, "The brain-computer interface based robot gives spinal cord injury patients a full-cycle active rehabilitation," in *2021 9th International Winter Conference on Brain-Computer Interface (BCI)*, 2021, pp. 1–5, https://doi.org/10.1109/BCI51272.2021.9385371.

[56] V. M. Gallón, S. M. Vélez, J. Ramírez, and F. Bolaños, "Comparison of machine learning algorithms and feature extraction techniques for the automatic detection of surface EMG activation timing," *Biomedical Signal Processing and Control*, vol. 94, p. 106266, 2024, https://doi.org/10.1016/j.bspc.2024.106266.

[57] H. Iqbal, J. Zheng, R. Chai, and S. Chandrasekaran, "Electric powered wheelchair control using user-independent classification methods based on surface electromyography signals," *Medical & Biological Engineering & Computing*, vol. 62, no. 1, pp. 167–182, 2024, https://doi.org/10.1007/s11517-023-02921-z.

[58] H. O. Shaw, K. M. Devin, J. Tang, and L. Jiang, "Evaluation of hand action classification performance using machine learning based on signals from two sEMG electrodes," *Sensors*, vol. 24, no. 8, p. 2383, 2024, https://doi.org/10.3390/s24082383.

[59] C.-T. Chang, Y.-C. Hsu, K.-J. Pai, C.-Y. Chou, and F.-H. Xu, "A myoelectric signal-driven intelligent wheelchair system incorporating occlusal control for assistive mobility," *Electronics*, vol. 14, no. 19, p. 3754, 2025, https://doi.org/10.3390/electronics14193754.

[60] E. Eddy, E. Campbell, S. Bateman, and E. Scheme, "Big data in myoelectric control: Large multi-user models enable robust zero-shot EMG-based discrete gesture recognition," *Frontiers in Bioengineering and Biotechnology*, vol. 12, p. 1463377, 2024, https://doi.org/10.3389/fbioe.2024.1463377.